The Astrophysical Journal, 563:546–554, 2001 December 20

ULTRALUMINOUS INFRARED GALAXIES: MERGERS OF SUB-L^* GALAXIES?

Luis Colina,[1] Kirk Borne,[2] Howard Bushouse,[3] Ray A. Lucas,[3] Michael Rowan-Robinson,[4] Andy Lawrence,[5] David Clements,[6] Amanda Baker,[6] and Seb Oliver[7]

Received 2001 February 8; accepted 2001 August 17

ABSTRACT

A sample of 27 low-redshift, mostly cool, ultraluminous infrared galaxies (ULIRGs) has been imaged at 1.6 μm with the *Hubble Space Telescope* (*HST*) Near-Infrared Camera and Multi-Object Spectrometer (NICMOS). The majority (67%) of the sample's galaxies are multiple-nucleus galaxies with projected separations of up to 17 kpc, and the rest of the sample (33%) are single-nucleus galaxies, as determined by the NICMOS angular resolution limit. The average observed, integrated (host + nucleus) H magnitude of our *HST* H sample ULIRGs is -24.3, slightly above that of an L^* galaxy ($M_H = -24.2$), and 52% of the sample's galaxies have sub-L^* luminosities. The ULIRGs in the *HST* H sample are not generated as a result of the merging of two luminous (i.e., $\geq L^*$) spiral galaxies. Instead, the interactions and mergers occur in general between two, or in some cases more, less massive sub-L^* (0.3–0.5L^*) galaxies.

Only one out of the 49 nuclei identified in the entire *HST* H sample has the properties of a bright quasar-like nucleus. On average, the brightest nuclei in the *HST* H sample galaxies (i.e., cool ULIRGs) are 1.2 mag fainter than warm ULIRGs and low-luminosity Bright Quasar Survey quasars (BQS QSOs) and 2.6 mag fainter than high-luminosity BQS QSOs. Since the progenitor galaxies involved in the merger are sub-L^* galaxies, the mass of the central black hole in these ULIRGs would be only about $(1–2) \times 10^7\ M_\odot$, if the bulge–to–black hole mass ratio of nearby galaxies holds for ULIRGs. The estimated mass of the central black hole is similar to that of nearby Seyfert 2 galaxies but at least 1 order of magnitude lower than the massive black holes thought to be located at the center of high-luminosity QSOs. Massive nuclear starbursts with constant star formation rates of 10–40 $M_\odot\ \mathrm{yr}^{-1}$ could contribute significantly to the nuclear H-band flux and are consistent with the observed nuclear H-band magnitudes of the ULIRGs in the *HST* H sample. An evolutionary merging scenario is proposed for the generation of the different types of ULIRGs and QSOs on the basis of the masses of the progenitors involved in the merging process. According to this scenario, cool ULIRGs would be the end product of the merging of two or more low-mass (0.3L^*–0.5L^*) disk galaxies. Warm ULIRGs and low-luminosity QSOs would be generated by a merger involving intermediate-mass ($0.5 < L < L^*$) spirals, or one L^* spiral with a less massive companion. High-luminosity QSOs would be the end point in the merging process of massive ($> L^*$) disk galaxies. Under this scenario, warm ULIRGs could still be the dust-enshrouded phases of UV-bright low-luminosity QSOs, but cool ULIRGs, which are most ULIRGs, would not evolve into QSOs.

Subject headings: galaxies: active — galaxies: interactions — galaxies: nuclei — galaxies: starburst — infrared: galaxies — quasars: general

1. INTRODUCTION

Ultraluminous infrared galaxies (ULIRGs), with bolometric luminosities [$L_{\mathrm{bol}} \sim L_{\mathrm{IR}}(8–1000\ \mu\mathrm{m}) \geq 10^{12}\ L_\odot$] comparable to those of quasars (QSOs), are the most luminous galaxies in the local universe, are extremely rich in the raw materials of star formation and owe their peculiar morphologies to strong interactions and mergers with other galaxies (see Sanders & Mirabel 1996 for a review) or even to multiple mergers (Borne et al. 2000).

Some investigators have proposed that ULIRGs represent the initial, dust-enshrouded stages of QSOs (Sanders et al. 1988) and also that these systems are forming elliptical galaxies through the dissipative collapse experienced during the final stages of a merging process (Kormendy & Sanders 1992). Therefore, according to these evolutionary scenarios, ULIRGs could be the progenitors of luminous QSOs embedded in elliptical galaxies. Recent studies of low-redshift QSOs and their environments indicate that a large fraction of these QSOs are involved in strong interactions or show close companions suggestive of recent interactions similar to those detected in ULIRGs (Bahcall et al. 1997 and references therein; Hutchings & Morris 1995; McLeod & Rieke 1995, 1999; Boyce et al. 1996, 1998; Boyce, Disney, & Bleaken 1999, McLure et al. 1999).

Mid-infrared spectroscopy with the *Infrared Space Observatory* has shown that ULIRGs with optical H II– and LINER-like spectra (i.e, about 80% of the ULIRGs) are dominated by the energy output from nuclear starbursts (Lutz et al. 1998; Genzel et al. 1998; Lutz, Veilleux, &

[1] Instituto de Física de Cantabria (CSIC-UC), Facultad de Ciencias, 39005 Santander, Spain; colina@ifca.unican.es.

[2] Raytheon Information Technology and Scientific Services, NASA Goddard Space Flight Center, Greenbelt, MD 20771; borne@rings.gsfc.nasa.gov.

[3] Space Telescope Science Institute, 3700 San Martin Drive, Baltimore, MD 21218; bushouse@stsci.edu, lucas@stsci.edu.

[4] Imperial College of Science, Technology and Medicine, Astrophysics Group, The Blackett Laboratory, London SW7 2BZ, UK; m.rrobinson@ic.ac.uk, s.oliver@ic.ac.uk.

[5] University of Edinburgh, Institute for Astronomy, Royal Observatory, Edinburgh EH9 3JZ, UK; a.lawrence@roe.ac.uk.

[6] Department of Physics and Astronomy, Cardiff University, P.O. Box 913, Cardiff, Wales, CF24 3YB, UK; a.baker@astro.cf.ac.uk, david.clements@astro.cf.ac.uk.

[7] Astronomy Centre, CPES, University of Sussex, Brighton BN1 9QJ, UK; S.Oliver@sussex.ac.uk.

Genzel 1999). However, the increased fraction of active galactic nuclei (AGNs) among the more luminous ULIRGs ($L_{IR} \geq 10^{12.3}\ L_\odot$) is taken as evidence for the presence of a dust-enshrouded QSO powering these galaxies, at least at the brightest end of the ULIRG luminosity distribution (Veilleux, Kim, & Sanders 1999).

A *Hubble Space Telescope* (*HST*) optical (*I*-band) survey of ULIRGs (120+ galaxies imaged; Borne et al. 2001, in preparation) has shown that fine structure is seen within a radius of less than 2″ for each galaxy. Only 11 galaxies (i.e., 9% of the sample) show a "stellar" nucleus, indicating the likely presence of a QSO-like nucleus. The subarcsecond morphology is chaotic, clumpy, and extended in the rest of the sample, suggestive of strong dust lanes and starburst activity. This indicates that distributed intense star-forming complexes represent the typical mode of star formation in these galaxies. Recent two-dimensional field spectroscopy of ULIRGs shows that optical emission lines trace regions located well outside the nuclei (Colina, Arribas, & Borne 1999; Arribas, Colina, & Clements 2001) and in some cases, with no direct relation to the dominant near-infrared nucleus and associated with extranuclear massive star-forming regions (Colina et al. 2000; Arribas, Colina, & Borne 2000).

Surveys at submillimeter wavelengths have recently discovered a large number of galaxies at high redshift (the so-called SCUBA sources at $z \sim 1$–4) showing properties similar to those of low-redshift ULIRGs (Smail, Ivison, & Blair 1997; Hughes et al. 1998; Barger et al. 1998; Barger, Cowie, & Sanders 1999; Eales et al. 1999; Blain et al. 1999). These galaxies could represent the primary epoch in the formation of spheroids and massive black holes triggered by interactions and mergers. As such, they represent a key stage in the evolutionary history of galaxies. Studies of samples of low-redshift ULIRGs, which appear to be local templates of the SCUBA sources, would therefore lead to a greater understanding of massive star formation, the formation of ellipticals and QSOs, the formation of globular clusters and possibly dwarf galaxies, and, in general, the formation and evolution of galaxies over cosmic time.

This paper presents the results derived from an imaging survey of a representative sample of low-redshift ULIRGs observed in the near-infrared with *HST*. Details on the sample are mentioned in § 2, while short comments about the observations, calibration, and photometric measurements are presented in § 3. The main results of the survey, including the characterization of ULIRGs, their magnitudes, light distribution, projected separations between the nuclei, etc., are presented in § 4. Finally, § 5 is devoted to a discussion of the evidence for/against the merger of two equal-mass bright spiral galaxies, and for/against dust-enshrouded QSOs. The similarities between ULIRGs and QSOs, and a possible evolutionary merger scenario, are also discussed. Section 6 summarizes the main results and conclusions drawn from this study.

2. THE *HST* ULTRALUMINOUS INFRARED GALAXY SAMPLE

We have been carrying out a multiwavelength *HST* snapshot imaging survey of ULIRGs. Our original sample for the *I*-band *HST* imaging survey consisted of 160 galaxies chosen from several published lists (the *HST I* sample; Borne et al. 2001, in preparation). A representative subsample of 50 galaxies was selected for the near-infrared snapshot survey, consisting of galaxies from the QDOT all-sky redshift survey of *IRAS* galaxies (Lawrence et al. 1999) and complemented with galaxies from the Melnick & Mirabel southern sky sample (Melnick & Mirabel 1990) and from the Clements sample (Clements et al. 1996). The final observed sample (hereafter the *HST H* sample) consists of 27 galaxies of which 17 are from the QDOT sample, nine from the Melnick & Mirabel sample, and one from the Clements sample. The optical and near-infrared *HST* images of all the galaxies in the sample as well as a short morphological description can be found in a separate paper (Bushouse et al. 2001).

The 27 ULIRGs in our sample have an average 60 μm luminosity $\log (L_{60}/L_\odot) = 12.02 \pm 0.19$ with a logarithmic luminosity distribution covering the range 11.7–12.5. Some investigators classify an infrared galaxy as ultraluminous when its luminosity integrated over the entire 8–1000 μm range (L_{IR}; see Sanders & Mirabel 1996 for the expression used to compute it) is above the $10^{12}\ L_\odot$ limit. However, many of the galaxies in our sample have only been detected at 60 μm, with upper limits to their 12 and 25 μm flux (see Bushouse et al. 2001 for a full listing of the fluxes). Therefore, we classify a bright infrared galaxy as ultraluminous when its 60 μm monochromatic luminosity (L_{60} defined as $\nu \times f_\nu$) is above the $10^{11.7}\ L_\odot$ limit. The reason for selecting this limit is that the integrated 8–1000 μm infrared luminosity (L_{IR}) is about 2 times the far-infrared luminosity (L_{FIR}) obtained using the *IRAS* 60 and 100 μm measurements for a wide range in dust temperatures (Helou et al. 1988), and it is about 3 times the 60 μm luminosity (L_{60}) in nearby nuclear starburst galaxies (L. Colina 1996, unpublished).

Of the 27 galaxies in the *HST H* sample, 22 (i.e., 81%) are classified as cool ULIRGs ($f_{25}/f_{60} < 0.2$), one (i.e., 4%) is a warm ULIRG, and four (i.e., 15%) cannot be classified until a measurement, and not an upper limit, of their 25 μm flux is obtained (see Table 2). The *HST* ULIRG sample covers a range in redshift from $z = 0.045$ to 0.301, with an average redshift of $z = 0.155 \pm 0.057$, similar to well-studied samples of low-redshift UV-bright low- and high-luminosity QSOs (LL-QSOs and HL-QSOs, respectively; $z = 0.106 \pm 0.031$, McLeod & Rieke 1994a; $z = 0.199 \pm 0.050$, McLeod & Rieke 1994b; $z = 0.194 \pm 0.051$, Bahcall et al. 1997) against which the results of this survey will be compared. Additional samples of low-redshift cool and warm ULIRGs (Surace, Sanders, & Evans 2000; Surace & Sanders 1999) are also included in the analysis.

3. OBSERVATIONS AND DATA ANALYSIS

3.1. *Observations and Basic Reductions*

Our near-infrared *HST* imaging survey utilizes camera 2 (NIC2) of the Near Infrared Camera and Multi-Object Spectrometer (NICMOS). The snapshot images were obtained with filter F160W (i.e., the *HST H*-band filter) to minimize the thermal background and therefore to increase the likelihood of detecting not only high surface brightness regions but also extended low surface brightness features associated with tidal tails and faint dwarf companions.

The total integration time of 640 s per ULIRG exposure consisted of four independent integrations of 160 s each and employed a square dithering pattern with a step of 3.″75. The dither pattern and its step size were selected in order to

increase the standard NIC2 field of view (19.″4 × 19.″3 with a pixel size of 0.″0759 × 0.″0752).

Full details on the calibration process are found in the atlas paper describing the morphology of the galaxies (Bushouse et al. 2001). Final images were mosaicked without performing any drizzling since the expected gain in resolution for NIC2 images is minimal.

3.2. *Photometric Measurements*

Aperture photometry was done on the final mosaicked and calibrated F160W images. The integrated count rate for a given aperture has been converted to magnitudes in the Vega system using the standard expression

$$M_H = -2.5 \times \log\,[\mathrm{PHOTFNU} \times \mathrm{DN} \times \mathrm{ZP(Vega)}^{-1}]\,, \quad (1)$$

where PHOTFNU = 2.07006×10^{-6} Jy s DN^{-1}, DN is the integrated count rate for a given aperture, and ZP(Vega) = 1113 Jy. The count rate–to–flux conversion factor gives an absolute photometry with an uncertainty of about 5% owing to the intrinsic uncertainties in the absolute flux of the spectral energy distributions of the primary NICMOS standards (one solar analog and one white dwarf) used in the calibration of NICMOS.[8]

Since the characteristics (effective wavelength and width) of the *HST* F160W filter are very similar to that of ground-based *H*-band filters, the *H* magnitudes given in this paper do not deviate by more than about 0.05–0.1 mag from ground-based *H* magnitudes. A Hubble constant $H_0 = 70$ km s^{-1} Mpc^{-1} and $q_0 = \frac{1}{2}$ are used throughout this paper to compute absolute *H*-band magnitudes and 60 μm luminosities.

4. NEAR-INFRARED CHARACTERIZATION OF ULIRGS

4.1. *Internal Extinction Corrections*

The absolute *H*-band magnitudes given in this paper are observed magnitudes, not corrected by internal extinction. Near-infrared colors of the nuclear regions of cool ULIRGs are consistent with line-of-sight extinctions of few magnitudes (2–5) in the visual (Scoville et al. 2000; Surace et al. 2000). Since extinction in the *H* band is 5.5 times less than in the visual, the dereddened nuclear *H*-band luminosity in our sample would therefore be increased by 0.4–0.9 mag. Two-dimensional optical extinction measurements of the nuclear and extended extranuclear ionized gas associated with some nearby cool ULIRGs like Mrk 273, IRAS 1211+0305, and Arp 220 (Colina et al. 1999, 2000; Arribas et al. 2001), and warm ULIRGs like IRAS 08572+3915 (Arribas et al. 2000) detect large absorption gradients with average extinction values equivalent to A_H of 0.1–0.3 mag, lower than the upper limit of about 1 mag mentioned above. Moreover, dereddening the observed luminosity in the nuclear regions increases the integrated (nucleus + host) galaxy luminosity typically by 0.1 mag, and only in extreme cases up to 0.4 mag (Surace et al. 2000). Therefore, independent measurements at optical and near-infrared wavelengths indicate that the average integrated *H*-band extinction over the entire size of the ULIRG system is small and amounts to about a few tenths of a magnitude. Consequently, the observed integrated and host absolute magnitudes are close to the real values since the dereddening corrections are small. On the other hand, the observed nuclear magnitudes could differ in some cases by about 1 mag.

4.2. *Integrated Absolute Magnitudes*

The integrated magnitude corresponds to that of the host galaxy plus the additional emission from the nucleus, likely dominated by the contribution of a nuclear starburst or of an AGN. The distribution of integrated *H* magnitudes for the *HST H* sample, mostly cool ULIRGs, is presented in Figure 1 (*upper left panel*). The sample's average is $M_H = -24.26 \pm 0.65$, in perfect agreement with the corresponding value obtained from a smaller and independent sample of cool ULIRGs from ground-based images (Surace et al. 2000; see also Table 2). For comparison, the warm ULIRG sample (Surace & Sanders 1999) is about 1 mag brighter ($M_H = -25.21 \pm 1.08$ for 10 galaxies without 3C273; see Table 2). All the warm ULIRGs in the Surace and Sanders sample are classified as Seyfert galaxies (about equally distributed among types 1 and 2), while the galaxies in our *HST H* sample for which a classification exists (55% of the sample) are classified either as starbursts, LINERs, mixed starbursts, or Seyfert 2. Only one galaxy (IRAS 20037−1547), which is the only warm ULIRG in the *HST H* sample, is classified as a Seyfert 1 (see Table 1 for the activity classification).

4.3. *Absolute Nuclear Magnitudes*

The nuclear magnitudes were obtained by measuring the total flux within an aperture having a distance-dependent angular diameter corresponding to 2.5 kpc (e.g., 1″ aperture at the average redshift of our sample). Previous near-infrared ground-based measurements used apertures with the same linear size, therefore making our measurements compatible with other published results (McLeod & Rieke 1994a, 1994b; Surace & Sanders 1999; Surace et al. 2000).

For galaxies having more than one nucleus (67% of the sample), two different cases have been considered: (1) a single measurement centered on the brightest nucleus was obtained for galaxies where the nuclei are separated by less than 2 kpc, and (2) two independent measurements, each centered on a different nucleus, were performed on galaxies where the projected nuclear separation is larger than 2 kpc. When more than two nuclei are present, as in the multiple-merger candidate galaxy IRAS 18580+6527 with six almost equally bright nuclei (see Bushouse et al. 2001 for a detailed description and optical and near-infrared images), only measurements centered on the two brightest nuclei are considered here (see Table 1 for results).

The distributions of *H*-band magnitudes for the brightest and second brightest nuclei are presented in Figure 1 (*upper middle and right panels*, respectively). The brightest nuclei have an average *H* magnitude of M_H(1st nucleus) = -23.2 ± 0.8, consistent with the value obtained for the Surace et al. (2000) sample of cool ULIRGs. The primary nuclei of the *HST H* sample's ULIRGs are therefore about 1 and 1.6 mag fainter than the nuclei of warm ULIRGs and LL-QSOs, and HL-QSOs, respectively (see values in Table 2).

Although differential extinction between the nuclei could affect their relative brightness in some systems, the secondary nuclei are on average, with a mean magnitude

[8] See the STScI NICMOS photometry Web page at http://www.stsci.edu/cgi-bin/nicmos for details and updates of the photometric parameters.

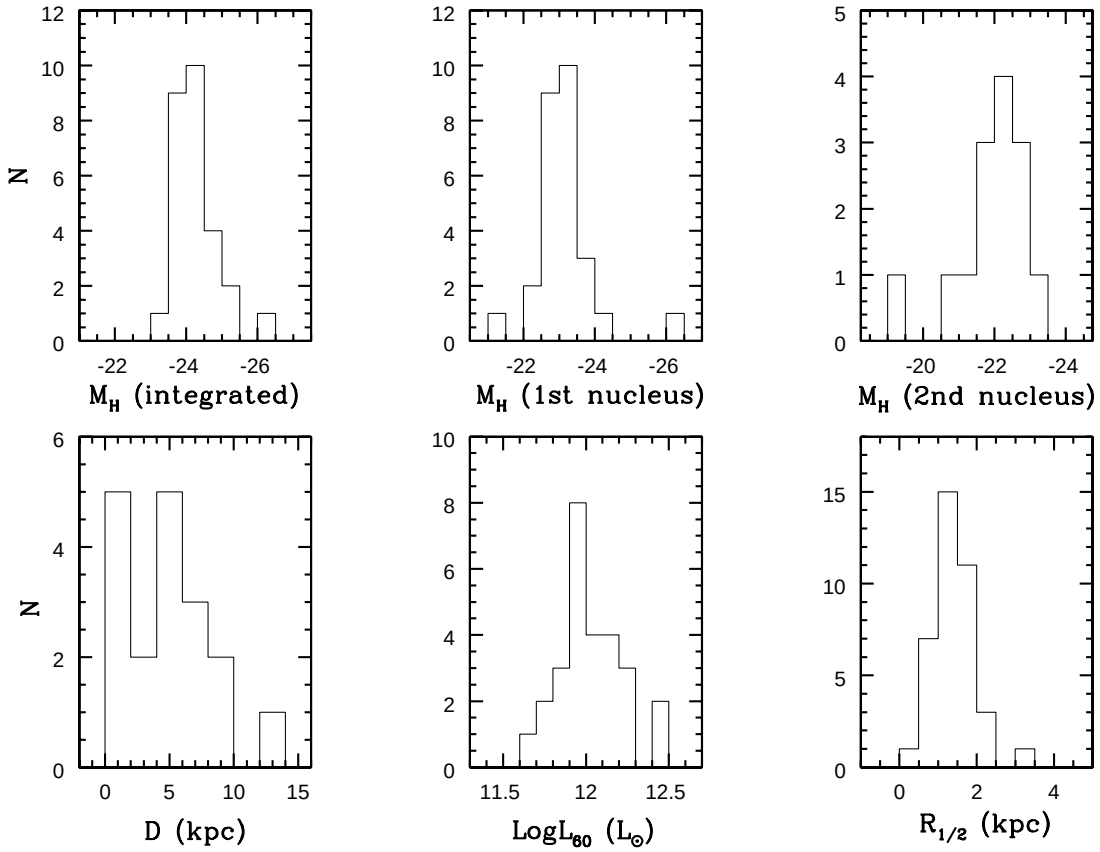

FIG. 1.—Distribution of the ULIRGs in the *HST H* sample according to their integrated *H* magnitudes (*upper left panel*), their brightest and second brightest nucleus (*upper middle and right panels*, respectively), their nuclear separation (*lower left panel*), their 60 μm luminosity (*lower middle panel*), and their *H*-band half-light radius (*lower right panel*). The absolute integrated magnitude (M_H) ranges from -23.0 to -26.3, with 70% of the ULIRGs in the range -23.5 to -24.5. The brightest nuclei [M_H(1st nucleus)] show a narrow distribution with 70% of the galaxies in the -22.5 to -23.5 range, while the secondary nuclei show a wider distribution. The sample shows a narrow distribution in the light concentration as given by the half-light radius ($R_{1/2}$) with 87% of the galaxies having values between 0.5 and 2.0 kpc. The nuclear separations of the double- or multiple-nucleus systems cover the range from 0.9 to 17 kpc, and about 33% of the sample's galaxies appear as single-nucleus systems.

M_H(2nd nucleus) $= -22.0 \pm 1.0$, about 3 times less luminous than the primary nucleus.

4.4. *Absolute Host Magnitudes*

The magnitude of the host galaxies has been obtained by taking out the contribution of the brightest nucleus (see § 4.3) from the integrated luminosity. The results are presented in Table 2. The magnitudes of the host galaxies obtained this way can be directly compared with those of samples of cool and warm ULIRGs (Surace et al. 2000; Surace & Sanders 1999), and luminous QSOs (McLeod & Rieke 1994a, 1994b). The absolute magnitude of the hosts ($M_H^{\rm host}$) ranges from -22.0 to -25.1, with 75% of the ULIRGs in the range -23.0 to -24.5. The sample's average is $M_H^{\rm host} = -23.6 \pm 0.7$, in agreement with the value derived for the smaller sample of cool ULIRGs for which ground-based data are available (Surace et al. 2000; see also Table 2). On the other hand, the host galaxies of warm ULIRGs and QSOs are more luminous. Warm ULIRGs and LL-QSO hosts are 0.7–0.8 mag brighter, while HL-QSO hosts are 1.4 mag brighter than the cool ULIRGs in our sample (see Table 2 for detailed values).

4.5. *Light Distribution and Pointlike Cores*

The light distribution for each galaxy in the *HST H* sample has been characterized by measuring its azimuthally averaged radial light profile and its corresponding half-light radius $R_{1/2}$ (the linear aperture radius containing half of the light). These measurements have been performed by centering on the brightest and second-brightest nuclei in an attempt to characterize the light distribution in the nuclear regions of ULIRGs ($\leq 4''$ in radius) and to quantify their compactness. For double- and multiple-nucleus galaxies, the measurements were done by first masking the other nucleus and then applying an ellipse-fitting algorithm to the light distribution. On average, the combined limitations of the signal-to-noise ratio and/or residual contribution from the masked nucleus restrict the fits to a radius $2''$ to $3''$ from the selected nucleus. The ellipse-fitting model does not take proper account of all the asymmetries in the overall light distribution present in these systems such as multiple nuclei, extended envelopes, and tidal tails. Therefore, the derived values for the half-light radius ($R_{1/2}$) are an estimate of the compactness of the light distribution in the *central* regions of the *HST H* sample galaxies. However, the half-light radius for the galaxies in the single-nucleus and multiple-nucleus subsamples are indistinguishable. This indicates that the light distribution in ULIRGs, even in multiple-nucleus systems, is extremely compact, and therefore the derived $R_{1/2}$ values will not change much, even if a full two-dimensional fit to the overall light distribution could be performed.

TABLE 1

PROPERTIES OF THE ULTRALUMINOUS INFRARED *HST H* SAMPLE GALAXIES

IRAS Object	z[a]	f_{25}/f_{60}	log L_{60}[b]	M_H[c]	M_H^{host}[d]	M_H^{1st}[e]	L_N/L_T[f]	M_H^{2ndg}	D[h]	Type[i]	Reference
03538−6432.....	0.3007	0.06	12.46	−25.33	−25.1	−23.6	0.20	−23.2	2.3	...	...
04413+2608.....	0.1712	<0.38	11.87	−24.77	−24.2	−23.8	0.42	−21.0	6.9	S2	1
05233−2334.....	0.1717	<0.11	11.69	−24.37	−23.6	−23.6	0.49	...	≤ 0.4	...	...
06206−6315.....	0.0918	0.07	12.00	−24.17	−23.8	−22.7	0.27	−22.2	4.1	S2	2
06268+3509.....	0.1698	<0.27	11.92	−24.47	−24.1	−23.1	0.28	−22.5	8.4	...	...
06361−6217.....	0.1596	0.10	12.11	−23.89	−23.1	−23.2	0.53	...	≤0.4	...	...
06561+1902.....	0.1882	<0.28	12.05	−24.08	−23.3	−23.4	0.51	−22.3	7.1	...	...
07381+3215.....	0.1703	<0.21	11.78	−24.14	−23.3	−23.5	0.55	...	≤0.4	...	...
10558+3845.....	0.2066	<0.15	11.92	−24.31	−24.0	−22.8	0.25	...	1.9	...	...
11095−0238.....	0.1061	0.13	12.04	−23.00	−22.7	−21.4	0.23	...	0.9	LI	2
13352+6402.....	0.2366	<0.08	12.24	−23.91	−22.7	−23.5	0.68	−21.7	12.3	...	...
13469+5833.....	0.1578	<0.06	11.99	−24.27	−23.9	−22.8	0.26	−22.2	4.1	H II	3
14378−3651.....	0.0682	0.08	11.92	−23.66	−22.5	−23.2	0.67	−19.2	5.0	S2	2
16159−0402.....	0.2126	0.31	12.14	−24.86	−24.1	−24.1	0.49	...	≤ 0.5	...	...
16455+4553.....	0.1906	0.09	12.03	−23.70	−22.6	−23.2	0.63	...	≤ 0.4	...	...
16541+5301.....	0.1936	<0.10	11.90	−24.72	−24.5	−23.0	0.20	−22.6	6.0	S2	1
18580+6527.....	0.1758	0.09	11.87	−25.12	−25.0	−22.7	0.10	−22.6	1.7−17	S2+H II	1
19297−0406.....	0.0856	0.08	12.19	−24.09	−23.8	−22.5	0.24	...	1.5	H II	4
20037−1547.....	0.1919	<0.17	12.28	−26.28	−24.5	−26.1	0.81	−23.0	6.4	S1	1
20087−0308.....	0.1034	0.05	12.20	−24.51	−24.0	−23.5	0.38	...	≤ 0.3	S2?LI	2
20100−4156.....	0.1291	0.07	12.42	−24.30	−23.9	−23.0	0.31	−21.6	5.9	H II>LI	2
20109−3003.....	0.1428	<0.28	11.72	−23.74	−23.2	−22.7	0.37	...	≤ 0.4	...	...
20176−4756.....	0.1781	0.09	11.93	−23.98	−23.3	−23.2	0.49	...	≤ 0.4	...	...
20414−1651.....	0.0871	0.08	11.99	−23.51	−22.5	−23.0	0.60	...	≤ 0.2	LI>H II	2
22206−2715.....	0.1330	<0.09	11.96	−24.27	−24.0	−22.6	0.21	−21.9	8.3	H II	3
23128−5919.....	0.0447	0.15	11.80	−23.81	−23.5	−22.2	0.23	−21.5	4.0	SB+LI+S2	2
23230−6926.....	0.1063	0.08	12.10	−23.80	−23.2	−22.9	0.45	...	1.0	LI+H II	2

[a] Redshift obtained from Lawrence et al. 1999, Clements et al. 1996, and Melnick & Mirabel 1990.
[b] 60 μm luminosity in units of $L_\odot$ computed for $H_0 = 70$ km s^{-1} Mpc^{-1} and $q_0 = \frac{1}{2}$ using the 60 μm flux densities from the *IRAS* Faint Source Catalog.
[c] Integrated H magnitudes within an aperture of 7.″5 in diameter (equivalent to 20 kpc at the mean redshift of the sample). For galaxies with particularly extended envelopes, tidal tails, or well-separated nuclei, larger apertures were used in order to include the more extended emission (11.″25 aperture for IRAS 06268+3509 and IRAS 22206−2715, and 15″ aperture for IRAS 06206−6315, IRAS 13352+6402, IRAS 18580+6527, and IRAS 23128−5919).
[d] H magnitude for the host galaxy obtained taking out the contribution of the brightest nucleus to the integrated luminosity.
[e] Nuclear H magnitude for the brightest nucleus.
[f] Fraction of nuclear to integrated total luminosity.
[g] Nuclear H magnitude for the second brightest nucleus.
[h] Separation in kpc between the brightest and second brightest nuclei.
[i] Activity class according to optical emission line ratios S1: Seyfert 1; S2: Seyfert 2; H II: Starburst; LI: LINER; a?b: no criterion to determine between types; a>b: two criteria favor type a and one b; a+b: divergent criteria.
REFERENCES.—(1) Lawrence et al. 1999; (2) Duc, Mirabel, & Maza 1997; (3) Veilleux et al. 1999; (4) Veilleux et al. 1995.

The single-nucleus galaxies make up 33% (9 out of 27) of the *HST* sample, while the rest of the sample (18 out of 27) contain either two nuclei within the same envelope (e.g., IRAS 11095−0238), several bright compact nuclei and extranuclear regions (e.g., IRAS 18580+6527), or extended emission peaks (giant H II regions or star-forming dwarf galaxies) around the main nucleus (e.g., IRAS 23128−5919) or in the tidal tails (e.g., IRAS 20100−4156). There are,

TABLE 2

PROPERTIES OF ULIRGS AND QSOS[a]

Sample	Redshift	M_H[b]	M_H^{host}[c]	$M_H^{nucleard}$	L_N/L_T	Reference
HST H Sample	0.155 ± 0.057	−24.26 ± 0.65	−23.6 ± 0.7	−23.2 ± 0.8	0.40 ± 0.18	1
HST COOL ULIRGs[e].....	0.150 ± 0.061	−24.23 ± 0.69	−23.6 ± 0.8	−23.1 ± 0.8	0.40 ± 0.20	1
COOL ULIRGs	0.091 ± 0.043	−24.25 ± 0.42	−23.7 ± 0.7	−23.0 ± 0.5	0.36 ± 0.17	2
WARM ULIRGs	0.126 ± 0.042	−25.21 ± 1.08	−24.4 ± 1.0	−24.2 ± 1.4	0.45 ± 0.20	3
LL-QSO	0.106 ± 0.031	−25.16 ± 0.46	−24.3 ± 0.5	−24.3 ± 1.0	0.55 ± 0.20	4
HL-QSO	0.199 ± 0.050	−26.27 ± 0.82	−25.0 ± 0.7	−25.8 ± 0.9	0.64 ± 0.13	5

[a] Absolute magnitudes for $H_0 = 70$ km s^{-1} Mpc^{-1} and $q_0 = \frac{1}{2}$. The absolute magnitude of an L^* galaxy is $M_H = -24.2$.
[b] Integrated (host plus nuclear) H-band magnitude.
[c] Absolute magnitude derived by subtracting the contribution of the nucleus (or brightest nucleus for double-nucleus systems) from the integrated H-band luminosity.
[d] Absolute magnitude of the nucleus, or brightest nucleus for double-nucleus systems.
[e] Average properties for the 22 ULIRGs from the *HST H* sample that are confirmed cool ULIRGs, i.e., already known to have $f_{25}/f_{60} < 0.2$.
REFERENCES.—(1) This work; (2) Surace et al. 2000; (3) Surace & Sanders 1999 without 3C 273; (4) McLeod & Rieke 1994a; (5) McLeod & Rieke 1994b.

however, no differences between the various morphological categories of *HST H* sample ULIRGs (for detailed descriptions see Bushouse et al. 2001) with regard to the half-light radius. The sample shows a narrow distribution in $R_{1/2}$ with an average half-light radius of 1.5 ± 0.5 kpc, equivalent to 0.″6 at the mean redshift of the sample (see Fig. 1, *lower right panel*).

Empirical evidence for the presence of bright, unresolved, pointlike sources (e.g., presence of diffraction spikes and Airy rings) has been obtained for 30% of the 27 systems imaged in our survey. At the average redshift of the *HST H* sample, these unresolved sources have a linear size of less than 0.4 kpc. The fraction of pointlike nuclei decreases to 16% if the total number of detected nuclei (49 considering the primary and secondary nuclei in double-nucleus systems and the six bright nuclei detected in IRAS 18580+6527) is considered. Of these, only one (IRAS 20037−1547) qualifies as a bright QSO-like nucleus, while the rest are a few magnitudes fainter than luminous QSOs (see discussion in § 5.1).

4.6. *Nuclear Separation*

Many ULIRGs in the sample show two bright nuclei within the same envelope. In some other cases, the two nuclei are well separated, and the bodies of two independent galaxies are still present. For all these ULIRGs (18 out of 27, or 67% of the sample), the linear separation of the nuclei has been established from the projected angular distance between the two brightest emission peaks, identified as the two nuclei, and neglecting any correction owing to the inclination of the orbital plane of the galaxies. In the few cases where more than two nuclei or bright compact condensations are present (IRAS 18580+6527 and IRAS 23128−5919), the nuclear separation is measured as the distance between the two brightest dominant emission peaks assumed to be the dynamically dominant components of the ULIRG system.

The nuclear separations of the double/multiple-nucleus systems in the *HST H* sample span the range from 0.9 to 17 kpc, with an average separation of 4.9 ± 3.1 kpc (Fig. 1, *lower left panel*). About 20% of the entire sample (i.e., five galaxies) have nuclear separations of less than 2 kpc and another 20% have separations between 4 and 6 kpc. Finally, the single-nucleus galaxies, representing 33% of the sample, could still have double nuclei separated by less than 0.4 kpc, i.e., the linear size corresponding to the *HST* NIC2 spatial resolution at the redshift of the single-nucleus galaxies.

5. DISCUSSION

5.1. *ULIRG Host Galaxies: Mergers of Two Equal-Mass L* Spirals?*

The morphological properties of ULIRGs (i.e., long tidal tails, double nuclei within common extended envelopes, close companions, large gas and dust content within regions a few kiloparsecs across, etc.) are consistent with the interaction/merger scenario where two gas-rich galaxies have already merged or are in the advanced stages of a merging process (see Borne et al. 2001, in preparation for an *HST* optical survey; see Barnes 1998 for models of strongly interacting galaxies). The timescale for the orbital decay of two merging nuclei owing to dynamical friction is given by $t_{\rm dyn} \sim (M_1/M_2)t_{\rm orb}$ (Carico et al. 1990), where M_1 and M_2 are the masses of the galaxies involved in the merging process. (Here we assume that the two galaxies are associated with the two brightest nuclei.) Assuming M_1/M_2 in the range 1–2, a typical orbital velocity of 250 km s^{-1}, and an average separation of 5 kpc, two disk galaxies in an advanced merging state and forming a ULIRG system would coalesce into a single-nucleus galaxy in less than 1.2×10^8 yr, while systems with the closest resolved nuclei (i.e., ≤ 2 kpc) would merge in less than 5×10^7 yr.

The unresolved single-nucleus *HST H* sample galaxies could still have double nuclei at distances of less than 0.4 kpc, implying a timescale of less than 10^7 yr for the merging and formation of a single nucleus. However, if the observed single-nucleus galaxies have already coalesced into a single nucleus and are the merger remnants of strong interactions between two Milky Way–type galaxies, their light profile would follow an $R^{1/4}$ law for about 8 mag with an effective radius of about 4 kpc (Barnes 1998). The light profile of some of the single-nucleus galaxies in the *HST H* sample are qualitatively consistent with this model's predictions; for example, IRAS 06361−6217 or IRAS 07381+3215 follow an $R^{1/4}$ law for about 6.5 mag but with a mean half-light radius of only 1.5 kpc, which is a factor of 2.5 smaller than predicted. This smaller half-light radius could be due to the presence of nuclear activity or to the fact that the progenitor galaxies were not luminous Milky Way–type galaxies but less luminous sub-L^* spirals (see below).

Even though the overall morphology of the ULIRGs in the *HST H* sample and the average separation of their multiple nuclei show that these galaxies are in the advanced phases of a merging process, their average integrated (host+nuclear) H magnitude ($M_H = -24.3$) argues against the hypothesis that the merging galaxies are two large (L^* or brighter) spiral galaxies. According to McLeod & Rieke (1994a), $M_H = -23.9$ for an L^* galaxy; adjusting to $H_0 = 70$ km s^{-1} Mpc^{-1}, this value corresponds to $M_H = -24.2$. Therefore, on average, the integrated luminosity of the merging galaxies that give rise to the cool ULIRGs in the *HST H* sample is equivalent to only one L^* galaxy. Moreover, 33% of the *HST H* sample ULIRGs have H-band integrated magnitudes in the -23.0 to -24.0 range, i.e., nucleus plus host luminosities less than L^* by a factor of 1.2–3. In normal, nonactive galaxies, the near-infrared continuum comes from the population of evolved red giants that dominates the stellar mass of the galaxy. However, in ULIRGs in general, nuclear starbursts dominate the energy output (Genzel et al. 1998), and consequently, the measured nuclear H-band magnitude is dominated by the contribution from massive red supergiants generated in the starbursts (see § 5.3). As a consequence, the integrated H magnitude gives an upper value to the true H-band magnitude of the ULIRGs' host galaxies.

A lower limit to the true luminosity of the host galaxy (labeled as $M_H^{\rm host}$ in Table 1) is derived by subtracting the contribution of the brightest nucleus from the integrated (nucleus+host) luminosity of the entire ULIRG system. The average H magnitude ($M_H^{\rm host} = -23.6$) corresponds then to an $0.6L^*$ galaxy. Thus, the average true H-band magnitude of cool ULIRGs lies between -23.6 and -24.3, i.e., between $0.6L^*$ and $1.1L^*$. Since most (67%) ULIRG systems in the *HST H* sample are in the advanced phases of a the merging process involving at least two galaxies (IRAS 18580+6527 is a candidate for a multiple merger; Borne et al. 2000), this result alone indicates that the merging

galaxies are not two equal-mass luminous ($\geq L^*$) gas-rich galaxies but rather a pair of faint sub-L^* ($0.3L^*$–$0.5L^*$) disk galaxies. This conclusion is valid even without dereddening corrections since internal dust absorption within the galaxies does not play a significant role in obscuring the integrated light of the host galaxies in the near-infrared (i.e., $A_H \sim 0.1$ mag; see discussion in § 4.1).

Our analysis of a large sample of cool ULIRGs (22 of the *HST H* sample systems are confirmed cool ULIRGs), complemented with the reanalysis of independent smaller samples of cool (13 galaxies; Surace et al. 2000) and warm ULIRGs (11 galaxies; Surace & Sanders 1999), disagrees with the conclusion given by these authors that the underlying host galaxies of cool and warm ULIRGs are essentially identical (average magnitudes according to our analysis are given in Table 2 for the three independent samples). Our analysis indicates that the hosts of warm ULIRGs (Surace & Sanders 1999) are, on average, a factor of 2 more luminous than the hosts of cool ULIRGs, covering also a wider range toward higher luminosities (Table 2 and notes). The host galaxies of cool ULIRGs have an upper limit of $2L^*$, while the hosts of warm ULIRGs with a bright pointlike Seyfert nucleus have luminosities well above this limit (Surace & Sanders 1999). If the *H*-band luminosity traces the mass in these systems, the luminosity difference between the warm and cool ULIRG hosts would imply that the galaxies involved in the merging process that generates ULIRGs cover a range in mass wider than previously thought. The differences in the absolute magnitude of the hosts can be interpreted as if mergers of intermediate-mass spirals ($0.5L^* < L < L^*$), or mergers involving at least one large L^* galaxy with a small companion, would produce QSO-like warm ULIRGs, while mergers of less massive spirals ($<0.5L^*$) would generate starburst-like cool ULIRGs. Under this scenario, not all ULIRGs would evolve into luminous UV-bright QSOs as suggested by some investigators (Sanders et al. 1988) but only the warm ULIRGs, where intermediate-mass gas-rich galaxies, or at least a large massive (L^*), were involved in the merging process. This scenario needs further investigation with a larger sample of warm ULIRGs.

5.2. *Nuclear Power Source in Cool ULIRGs: Dust-enshrouded QSOs?*

The qualitatively evolutionary scenario outlined by Sanders et al. (1988) proposed that ULIRGs are the initial, dust-enshrouded phases of QSOs, where the standard QSO UV-bright phase shows up only after the dense nuclear and circumnuclear interstellar media have been cleared out by the AGN-related outflows.

The increased fraction of Seyfert nuclei among the brightest ULIRGs [$L_{\rm IR}(8\text{–}1000\ \mu{\rm m}) \geq 10^{12.3}\ L_\odot$] is taken as evidence for the presence of a dust-enshrouded QSO powering these galaxies, at least at the brightest end of the ULIRG luminosity distribution (Veilleux et al. 1999). Is there any evidence for the existence of a dust-enshrouded QSO in our *HST H* sample ULIRGs?

Of the 27 systems in our *HST H* sample with a total of 49 detected nuclei, only one nucleus (IRAS 20037−1547) has the right set of properties to qualify as a QSO: (1) bright unresolved stellar-like source in the NICMOS image, (2) a near-infrared nuclear luminosity ($M_H = -26.05$) typical of Bright Quasar Survey (BQS) HL-QSOs (Table 2), and (3) the optical spectral characteristics of a Seyfert 1 (Lawrence et al. 1999). The rest of the *HST* ultraluminous galaxies for which an activity classification exists in the optical (15 out of 27 systems; see Table 1 for details), show the spectral characteristics of starbursts, LINERs, Seyfert 2, or mixed classifications, but no evidence for a Seyfert 1 nucleus. Moreover, of the five galaxies with IR luminosities ($L_{\rm IR}$) above the $10^{12.3}\ L_\odot$ limit and for which a spectral classification is available (IRAS 19297−0406, IRAS 20037−1547, IRAS 20087−0308, IRAS 20100−4156, and IRAS 23230−6926), only one, the already mentioned IRAS 20037−1547, is classified as a Seyfert 1 (see Table 1).

In addition, the brightest nuclei in the *HST H* sample are on average 3–10 times less luminous than LL-QSOs and HL-QSOs in the low-redshift BQS (McLeod & Rieke 1994a, 1994b), respectively (see Fig. 2 and Table 2). Also, the brightest nuclei in the *HST H* sample contain on average 40% of the total flux (L_N/L_T), while the LL-QSOs and HL-QSOs contain 55% and 64% of the total flux of their host + QSO systems, respectively (see Table 2 and Fig. 2).

These results suggest that either QSOs do not exist in general in the nuclear regions of the *HST H* sample

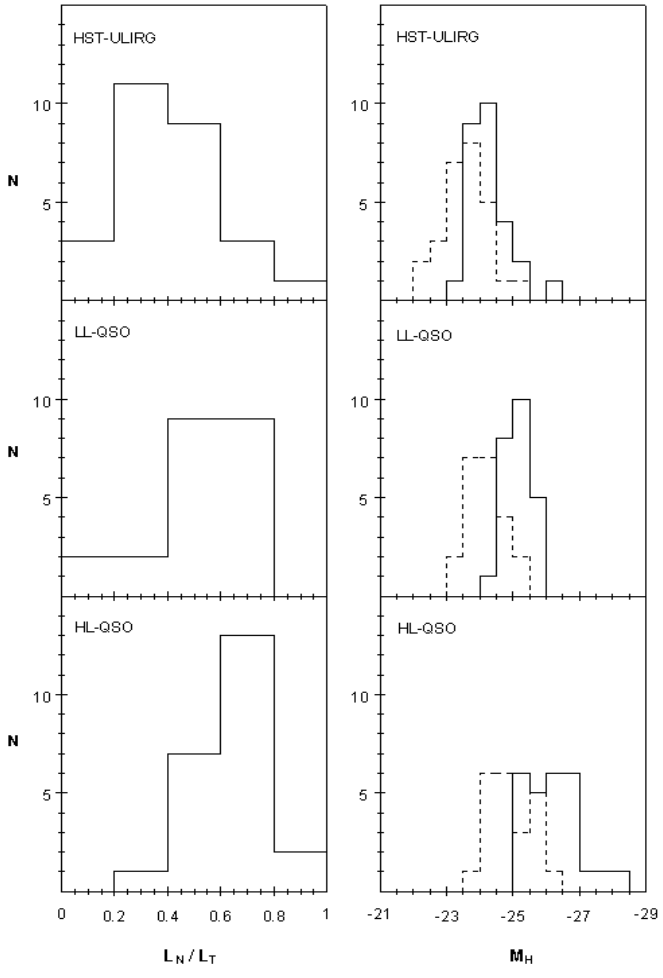

FIG. 2.—Comparison of the ULIRGs in the *HST H* sample with the BQS LL-QSO and HL-QSO samples (McLeod & Rieke 1994a, 1994b). The distribution of the *HST H* sample according to their integrated *H* magnitude (*solid line*) and to their fraction of nuclear to integrated light (L_N/L_T) are given in the upper left and right panels, respectively. The corresponding distributions for the LL-QSOs and HL-QSOs are also given in the middle and lower panels, respectively (*solid lines*). The *H* magnitude of the *HST H* sample (*HST*-ULIRG), LL-QSO, and HL-QSO host galaxies is also given in the same panels for comparison (*dotted lines*).

ULIRGs or that the QSOs are completely enshrouded in dust and are therefore not visible at near-infrared wavelengths. If the latter were the case, the average difference in the observed nuclear magnitude between the *HST H* sample nuclei and the LL-QSO and HL-QSO samples would imply H-band extinctions (A_H) of 1.2–2.6 mag, equivalent to visual nuclear extinctions (A_V) of 7–16 mag. These estimates are consistent with the extinction measurements based on mid-infrared line ratios [A_V(screen) $\sim$ 5–50 mag; Genzel et al. 1998]. However, near-infrared *HST* colors of cool ULIRGs are consistent with starlight with a few magnitudes of visual extinction, therefore not favoring the presence of dust-enshrouded QSOs (Scoville et al. 2000; see also § 4.1).

Moreover, the progenitor galaxies involved in the collision and merging process giving rise to cool ULIRGs are gas-rich galaxies less massive than an L^* galaxy by factors of 2–4, on average (§ 5.1). If these galaxies follow the same bulge–to–black hole mass relation as measured in nearby spirals and ellipticals (Magorrian et al. 1998; Gebhardt et al. 2000; Merritt & Ferrarese 2001), the expected mass of the central black hole will be about (1–2) $\times$ 10^7 $M_\odot$, similar to that of nearby Seyfert 2 or LINER type galaxies (Ho & Kormendy 2001) but at least 1 order of magnitude smaller that the massive black holes in luminous QSOs.

In summary, the empirical arguments based on (1) the nondetection of bright QSO-like nuclei (only one in 49 nuclei has the compactness and luminosity of a QSO nucleus), (2) the H-band absolute nuclear magnitudes, and (3) the integrated H-band magnitude of the ULIRG host galaxies, complemented, when available, with spectral classifications, do not support the presence of dust-enshrouded QSOs in the nuclei of cool ULIRGs, not even at the brightest end of the luminosity function [i.e., $L_{\rm IR}$(8–1000 μm) $\geq$ $10^{12.3}$ $L_\odot$]. High spatial resolution mid-infrared imaging of a large sample of cool ULIRGs is needed to establish this conclusion on a more firm footing.

5.3. *Nuclear Power Source in Cool ULIRGs: Massive Nuclear Starbursts?*

The near-infrared energy output of the bulges of nonactive disk galaxies comes from the old, evolved stellar population (i.e., red giants). Since ULIRGs are mergers of disk galaxies, the bulges of the progenitor galaxies could contribute significantly to the nuclear H-band flux emitted in the nuclear regions. However, many of the ULIRGs in the *HST H* sample, as well as ULIRGs in general, are classified as starbursts or LINERs and therefore a considerable amount of their nuclear near-infrared output should come from massive red supergiants associated with nuclear starbursts. In particular, red supergiants produced in massive starbursts with a continuous star formation rate contribute 80%–90% of their near-infrared luminosity (M. Mas-Hesse & M. Cerviño 2000 private communication).

On average, the first and second brightest nuclei in the *HST H* sample ULIRGs have magnitudes $M_H = -23.2$ and -22.0, respectively. For comparison, a 2×10^7 yr old continuous starburst characterized by a Salpeter initial mass function and forming 1–100 $M_\odot$ stars at a rate of 10–20 $M_\odot$ yr^{-1} (equivalent to a rate of 25–50 $M_\odot$ yr^{-1}, if stars in the range of 0.1–100 $M_\odot$ were formed), has an absolute H-band magnitude M_H(burst) $\sim$ -21.7 to -22.5 (Leitherer et al. 1999). Thus, the observed H nuclear magnitudes of the first and second brightest nuclei are consistent with massive nuclear starbursts with a continuous star formation rate of about 10–40 $M_\odot$ yr^{-1}, respectively. These star formation rate estimates are compatible with the values derived from the infrared luminosity. More massive nuclear starbursts could still be present if internal extinctions amounting to a few tenths magnitudes in the near-infrared are considered.

5.4. *ULIRGs and QSO Host Galaxies*

Recent *HST* images of QSOs (Bahcall et al. 1997 and references therein; Hutchings & Morris 1995; McLeod & Rieke 1995, 1999; Boyce et al. 1996, 1998, 1999; McLure et al. 1999) have shown that QSOs live in very different environments, with many of them involved in interaction or merging processes. Focusing on the results from a representative sample of QSOs (Bahcall et al. 1997) covering a redshift similar to that of our *HST* ULIRG sample, most of the QSOs (50%) are hosted by normal ellipticals, but a large fraction (25%) of QSOs appear to be in complex interacting systems, and another 15% are located in spiral galaxies with H II regions. Also, representative samples of radio-loud and radio-quiet QSOs imaged with *HST* have a large interaction fraction with about 75% of the QSOs showing the morphological characteristics (tidal tails, close companions, double nuclei) associated with galaxy interactions (McLure et al. 1999). These fractions are very similar to those obtained for our *HST H* sample where 67% of the ULIRGs have double or multiple nuclei, about 33% are single-nucleus galaxies with elliptical-like light profiles, 11% still have some evidence of spiral arms, and basically all galaxies show the morphological signs of interactions or merging in their starlight distribution.

The observed morphological characteristics support that the different types of ULIRGs and QSOs are generated during the advanced phases, or even the final stages, in the interaction and merging of at least two gas-rich galaxies. The range covered by their hosts in absolute magnitude indicates that the galaxies involved in these interactions are not always massive and luminous ($\geq L^*$) galaxies. The host galaxies of cool ULIRG systems are, on average, sub-L^* galaxies (see § 5.1), about 2 times fainter than the hosts of warm ULIRGs and BQS LL-QSOs, and about 4 times fainter than the hosts of BQS HL-QSOs (Table 2). The average luminosities of the hosts of warm ULIRGs and of BQS LL-QSOs are similar, and slightly above that of an L^* galaxy. Finally, hosts of BQS HL-QSOs have, on average, luminosities corresponding to $2L^*$ galaxies.

Under the evolutionary merging hypothesis, cool ULIRGs would be generated during the merging of two or more low-mass sub-L^* (typically $0.3L^*$–$0.5L^*$) spirals, warm ULIRGs, and LL-QSOs in the merging of an L^* spiral with a substantially less massive sub-L^* disk galaxy (McLeod & Rieke 1994a), or during the merging of intermediate-mass ($0.5L^* < L < L^*$) spirals, and HL-QSOs in the merging of massive ($> L^*$) disk galaxies. Under this scenario, warm ULIRGs could still be the dust-enshrouded phases of UV-bright LL-QSOs, but cool ULIRGs, which represent most ULIRGs, would not evolve into QSOs.

6. SUMMARY

This paper has presented the results of a near-infrared survey of a sample of 27 low-redshift ultraluminous infrared galaxies imaged with the *HST* near-infrared camera (the

HST H sample). The main conclusions of this study are as follows:

1. The vast majority (22 out of 27, or 81%) of the galaxies in the *HST H* sample are cool ULIRGs with only one warm ULIRG and four galaxies still pending their classification. The *HST H* sample represents the largest sample of ULIRGs imaged with high spatial resolution in the near-infrared.

2. The majority (67%) of the ULIRGs have two or more nuclei, some of them within a common envelope. The rest of the sample's galaxies (33%) are single-nucleus galaxies, at the resolution of *HST*.

3. The two brightest nuclei in the double/multiple-nucleus systems are separated by up to 17 kpc, with an average separation of 5 kpc, and with the nuclei in 20% of the sample's galaxies separated by less than 2 kpc. The average dynamical time for the double-nucleus galaxies to coalesce into a single nucleus owing to dynamical friction is less than 1.2×10^8 yr.

4. Single-nucleus galaxies could still have double nuclei with a separation of less than 0.4 kpc. If this were the case, the nuclei would be merging in less than 2×10^7 yr.

5. 52% of the *HST H* sample's ULIRGs have integrated H magnitudes corresponding to sub-L^* galaxies, while the average of the sample (-24.26 ± 0.65) corresponds to that of an L^* galaxy (-24.2). These results do not favor the scenario where the interaction and merging of two luminous (i.e., $\geq L^*$) spiral galaxies generate cool ULIRGs but supports instead the interaction and merger of two, or more, $0.3L^*$–$0.6L^*$ galaxies.

6. Since the progenitor galaxies of the cool ULIRGs are sub-L^* galaxies, the mass of their central black hole would be about (1–2) $\times 10^7\ M_\odot$, if the black hole–to–bulge mass relation found in nearby ellipticals and spirals holds for ULIRGs. This mass is consistent with that of LINERs and Seyfert 2 nuclei but is a factor of 10 smaller than the expected in UV-bright luminous QSOs.

7. There is no evidence for dust-enshrouded QSOs in our sample of ULIRGs. Only one out of the 49 nuclei identified in the entire sample, which is located in a warm ULIRG, has the properties characteristic of luminous QSOs. Moreover, the brightest nuclei of the *HST H* sample ULIRGs are on average 1.2 and 2.6 mag fainter than the low-redshift BQS LL-QSOs and HL-QSOs, a difference not accounted for by internal extinction effects. Moreover, the observed nuclear H-band magnitudes for the brightest and second brightest nuclei are consistent with 40 and 10 $M_\odot\ \mathrm{yr}^{-1}$ nuclear starbursts, respectively.

8. An evolutionary merging scenario is proposed for the different types of ULIRGs and QSOs on the basis of the masses of the progenitors involved in the interaction and merger. According to this scenario, cool ULIRGs would represent the advanced phases in the merging of two or more sub-L^* ($<0.5L^*$) galaxies, warm ULIRGs and LL-QSOs would be generated during the merger of intermediate-mass ($0.5L^* < L < L^*$) spirals, and HL-QSOs would be the final product in the merging of massive ($>L^*$) disk galaxies. Under this scenario, warm ULIRGs could still be the dust-enshrouded phases of UV-bright LL-QSOs, but cool ULIRGs, which represent most ULIRGs, would not evolve into luminous QSOs.

Luis Colina thanks the Space Telescope Science Institute (STScI) for financial support through its Collaborative Visitor Program. Support for this work was provided by CICYT (Comisión Inerministerial de Ciencia y Tecnología) through grant PB98-0340-C02-02 and by NASA through grant GO-06346.01-95A from STScI.

REFERENCES

Arribas, S., Colina, L., & Borne, K. 2000, ApJ, 545, 228
Arribas, S., Colina, L., & Clements, D. 2001, ApJ, 560, 160
Bahcall, J. N., Kirhakos, S., Saxe, D. H., & Schneider, D. P. 1997, ApJ, 479, 642
Barger, A. J., Cowie, L. L., & Sanders, D. B. 1999, ApJ, 518, L5
Barger, A. J., Cowie, L. L., Sanders, D. B., Fulton, E., Taniguchi, Y., Sato, Y., Kawara, K., & Okuda, H. 1998, Nature, 394, 248
Barnes, J. E. 1998, in Galaxies: Interactions and Induced Star Formation, ed. D. Friedli, L. Martiner, & D. Pfenniger (Saas-Fée Advanced Course 26; Berlin: Springer), 275
Blain, A. W., Smail, I., Ivison, R. J., & Kneib, J.-P. 1999, MNRAS, 302, 632
Borne, K., Bushouse, H., Lucas, R. A., & Colina, L. 2000, ApJ, 529, L77
Boyce, P. J., et al. 1996, ApJ, 473, 760
———. 1998, MNRAS, 298, 121
Boyce, P. J., Disney, M. J., & Bleaken, D. G. 1999, MNRAS, 302, L39
Bushouse, H., et al. 2001, ApJS, in press
Carico, D. P., Graham, J. R., Matthews, K., Wilson, T. D., Soifer, B. T., Neugebauer, G., & Sanders, D. B. 1990, ApJ, 349, L39
Clements, D. L., Sutherland, W. J., Saunders, W., Efstathiou, G. P., McMahon, R. G., Maddox, S., Lawrence, A., & Rowan-Robinson, M. 1996, MNRAS, 279, 459
Colina, L., Arribas, S., & Borne, K. 1999, ApJ, 527, L13
Colina, L., Arribas, S., Borne, K., & Monreal, A. 2000, ApJ, 533, L9
Duc, P. A., Mirabel, I. F., & Maza, J. 1997, A&AS, 124, 533
Eales, S., Lilly, S., Gear, W., Dunne, L., Bond, J. R., Hammer, F., Le Fevre, O., & Crampton, D. 1999, ApJ, 515, 518
Gebhardt, K., et al. 2000, ApJ, 539, L13
Genzel, R., et al. 1998, ApJ, 498, 579
Helou, G., Khan, I. R., Malek, L., & Boehmer, L. 1988, ApJS, 68, 151
Ho, L. C., & Kormendy, J. 2001, in Encyclopedia of Astronomy and Astrophysics (Bristol: Inst. Phys. Publ.)
Hughes, D. H., et al. 1998, Nature, 394, 241
Hutchings, J. B., & Morris, S. C. 1995, AJ, 109, 1541
Kormendy, J., & Sanders, D. B. 1992, ApJ, 390, L53
Lawrence, A., et al. 1999, MNRAS, 308, 897
Leitherer, C., et al. 1999, ApJS, 123, 3
Lutz, D., Spoon, H. W. W., Rigopoulou, D., Moorwood, A. F. M., & Genzel, R. 1998, ApJ, 505, L103
Lutz, D., Veilleux, S., & Genzel, R. 1999, ApJ, 517, L13
Magorrian, J., et al. 1998, AJ, 115, 2285
McLeod, K. K., & Rieke, G. H. 1994a, ApJ, 420, 58
———. 1994b, ApJ, 431, 137
———. 1995, ApJ, 454, L77
———. 1999, ApJ, 511, L67
McLure, R. J., Kukula, M. J., Dunlop, J. S., Baum, S. A., O'Dea, C. P., & Hughes, D. H. 1999, MNRAS, 308, 377
Melnick, J., & Mirabel, I. F. 1990, A&A, 231, L19
Merritt, D., & Ferrarese, L. 2001, ApJ, 547, 140
Sanders, D., & Mirabel, I. F. 1996, ARA&A, 34, 749
Sanders, D., Soifer, B. T., Elias, J. H., Madore, B. F., Matthews, K., Neugebauer, G., & Scoville, N. Z. 1988, ApJ, 325, 74
Scoville, N. Z., et al. 2000, AJ, 119, 991
Smail, I., Ivison, R. J., & Blain, A. W. 1997, ApJ, 490, L5
Surace, J. A., & Sanders, D. B. 1999, ApJ, 512, 162
Surace, J. A., Sanders, D. B., & Evans, A. S. 2000, ApJ, 529, 170
Veilleux, S., Kim, D. C., & Sanders, D. B. 1999, ApJ, 522, 113
Veilleux, S., Kim, D. C., Sanders, D. B., Mazzarella, J. M., & Soifer, B. T. 1995, ApJS, 98, 171